Journal of Atmospheric Pollution, 2016, Vol. 4, No. 1, 23-29
Available online at http://pubs.sciepub.com/jap/4/1/3

DOI:10.12691/jap-4-1-3

Ecological Evaluation of Urban Heat Island in Chicago City, USA

R. Alfraihat, G. Mulugeta, T. S. Gala*

Department of Geography, Chicago State University, Chicago, IL., USA
*Corresponding author: tgala@csu.edu

Abstract The city of Chicago has experiences of Urban Heat Island (UHI) phenomena and a good example is its widely reported heat wave of 1995. This study conducted an ecological evaluation of Chicago's UHI phenomena using LANDSAT TM of 2010, almost 15 years after the lethal heat wave and subsequently implemented various UHI mitigation efforts. The thermal characteristics of the city were assessed with a Land Surface Temperature (LST), a parameter retrieved from LANDSAT TM 6; a thermal-infrared (TIR) band (10.40 to 12.50μm), using mono-window algorithm. The ecological evaluation was made using an Urban Thermal Field Variance Index (UTFVI), which quantitatively evaluated the UHI effects on the quality of urban life. The accuracy of the model was assessed against theoretical relationships between the LST, the Normalized Difference Vegetation Index (NDVI), and Normalized Difference Built-up Index (NDBI). The LST of Chicago ranges from 18^{o}C in Urban Cool Islands (UCI) to 44^{o}C in UHI. In Chicago, although the cooling effects of Lake Michigan, downtown's sky-high buildings, and urban parks and green spaces have worked together to suppress the concerns of UHI effects locally, still some areas experience a high UHI. In general, 25% of the city experiences ecologically bad or worse UHI effects, indicating a need for continued UHI mitigation efforts.

Keywords: *Urban Heat Island (UHI), Ecological Evaluation of UHI Effects, Land surface temperature (LST), Urban Thermal Field Variance Index (UTFVI), Thermal Remote Sensing, Chicago Illinois*

Cite This Article: R. Alfraihat, G. Mulugeta, and T. S. Gala, "Ecological Evaluation of Urban Heat Island in Chicago City, USA." *Journal of Atmospheric Pollution*, vol. 4, no. 1 (2016): 23-29. doi: 10.12691/jap-4-1-3.

1. Introduction

The global growing expanse of cities and towns has now reached a stage where over 54% of the global population lives in urban areas [1,2]. According to 2014 Revision of World Urbanization Prospects, this proportion will continue to grow and by 2050, cities' population is expected to increase to 66% of the world's population, or 5 billion people. Ninety percent of this growth will be in developing countries. There is a predictable change in the urban environment as a consequence of this growth. One such change in urban climates particularly is the formation of Urban Heat Islands (UHI), a situation where the cities' or metropolitan areas' ambient temperature is dramatically altered and become warmer than the surrounding rural areas [3,4]. The UHI affects urban quality of life through its impacts on human health, ecosystem function, local weather and climate. There is a direct relationship between peak UHI intensity and heat-related illness and fatalities [4,5].

The city of Chicago has experienced a high rate of population growth and urbanization [6,7,8]. According to census data, from 1990–2000 the population of metro Chicago increased by 11.58% and though the rate has declined in the subsequent decade, i.e., between 2000 and 2010, the metropolitan population was still growing at the rate of 3.86% [8]. The population growth has led to urbanization that resulted in significant land transformation. Accordingly, between 1989 and 2010 the urbanized area of Chicago has increased by 82.2%, which is associated with a loss of 25.8% of agricultural lands and a 32.5% decline in the urban open and green spaces [8]. Such land transformation has caused noticeable climate changes, including increased energy demands and air pollution thereby impacting the quality of urban life [9]. A good example is the great Chicago heat wave of 1995 that led to approximately 750 heat-related deaths in the city, 3300 excess emergency department visits, and a number of intensive care unit admissions for near-fatal heat stroke [10,11].

Several studies have dedicated their work to Chicago's UHI phenomenon [6,7,12,13]. Accordingly, using 20 years of records, a study [12] investigated point-based diurnal and seasonal variation and documented increased air temperature of the city by 1.85°C vis-à-vis surrounding rural areas. On the other hand, another study [13] evaluated the potential of green roofing technologies and found a reduced urban air temperature by 3°C, owing to increased albedo and evaporative cooling. Similarly, an investigation of the effectiveness of 15 years of UHI mitigation policies demonstrates spatially-resolved significant policy implications on the city's albedo and resultant cooling [6]. Furthermore, the variables from remote sensing and meteorology were combined to explain UHI phenomenon in 8 Chicago neighborhoods and reported the varying importance of time of the day on

overall efficiency of the city's UHI mitigation efforts [7]. However, a spatially-resolved ecological evaluation UHI effects with an Urban Thermal Field Variance Index (UTFVI) is pending for the city of Chicago.

Therefore, the objectives of this study were: a) to retrieve LST using LANDSAT- 6 TM images for the year 2010 and analyze the city's UHI phenomenon; and b) to carry out an Urban Thermal Field Variance Index (UTFVI) and identify areas that are subjected to greater risks of weather anomalies. Satellite remote sensors, especially those capacitated to detect thermal energy emitted from the earth's surface, are viable tools for large scale UHI studies. The tool is capable of estimating surface temperature to conduct UHI analysis [6] (e.g., Mackey, 2012) and of conducting ecological evaluations of UHI phenomena [14,15].

2. Material and Methods

2.1. Description of the Study Area

The City of Chicago is located in northeast Illinois, on the southern tip of Lake Michigan (Figure 1). Stretched over a geographical area of 234.0 sq mi (606 km^2), it has 2.7 million residents, which makes it the most populous city in both the U.S. state of Illinois and the American Midwest (US Census, 2014). The largest portion of Chicago's urban fabric is vegetative land cover, constituting almost 40% of the landscape. It has a paved surface of 31%, and total roofed area of 27% [17]. Not all roofs are colored to enhance albedo (i.e., reflection of solar radiations).

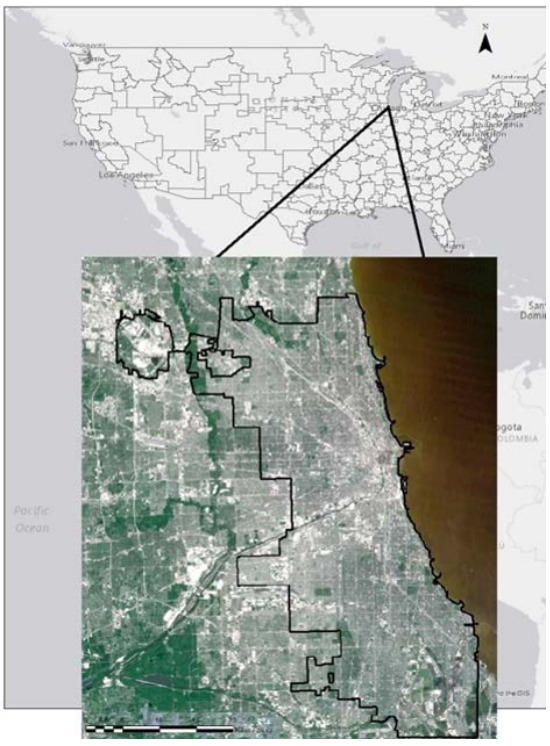

Figure 1. The study area, Chicago

Climatewise, the city lies within the humid continental climate. However, the flat terrain of Chicago and Lake Michigan make it has uniquely unpredictable and frequently extreme weather conditions. Average monthly temperatures for Chicago range from -6°C in January to 23°C in July. In general, summers are very hot and the highest temperatures of July and August could exceed 35°C, whereas winters are cold and snowy with few sunny days. The normal January's high is just below freezing. Spring and autumn are mild seasons with low humidity. The lake provides a positive effect, moderating Chicago's climate, thereby making waterfront areas warmer in winter and cooler in summer.

2.2. Data

Two major data were needed to conduct this research: satellite and meteorological data. A satellite image was obtained from the U.S. Geological Survey GLOVIS website via http://glovis.usgs.gov. The image was selected based on their good quality mainly in terms of cloud cover, date, month and year of collection (See Table 1). In terms of cloud cover, the image having 0% cloud cover was selected. This was to avoid possible impacts of clouds in data interpretation. U.S. Geological Survey supplies image(s) after geo-referencing them to the Universal Transverse Mercator (UTM), map projection (Zone 37), WGS 84 datum and ellipsoid. The detailed descriptions of the satellite images selected are specified in Table 1.

Table 1. Specifications of the satellite data used

Items	Specifications	
Date of Acquisition months/Day/Year	06/15/1995	09/12/2010
Time	15:41 Hrs.	16:56 Hrs.
Cloud cover	0%	2%
Resolution for Thermal Band 6	120 * 120m	120 * 120m
Path/row	23/31	23/31
Projection	UTM (Universal Transverse Mercator). Zone 16	UTM (Universal Transverse Mercator). Zone 16

Weather records corresponding to the same time the LANDSAT image was acquired are needed for the algorithms used to derive the LST. These are relative humidity, dew points, and atmospheric temperatures. The weather data were acquired from The Weather Channel Interactive Inc. website via http://www.wunderground.com/. Additionally, water vapor content in the air was among the required parameters for the LST modeling. The water vapor content was calculated as a function of Relative Humidity (RH) and near surface temperature (T^o) [15].

2.3. Methodology

Several algorithms are available for retrieving the LST, a key parameter for the UHI estimation. These are mono-window algorithm [20,21]; the split-window algorithm; temperature-emissivity separation algorithm [21] and the single-channel method [23]. While the split-window and temperature-emissivity separation algorithms are primarily developed for the Advanced Spaceborne Thermal Emission and Reflection Radiometer (ASTER) data, both the mono-window and single-channel algorithms are applicable for thermal LANDSAT data, of which the mono-window algorithm is relatively simple and highly effective for retrieving the LST for the analysis of the UHI [18]. Three fundamental activities were conducted to quantitatively evaluate the ecological effects of the UHI in Chicago. These were a) deriving a Normalized Difference Vegetation Index (NDVI) and a Normalized Difference

Built-up Index (NDBI) images; b) retrieving the LST using LANDSAT TM6 image of 2010 and analyzing the city's UHI phenomenon; and c) calculating the Urban Thermal Field Variance Index (UTFVI) and interpreting the ecological valuation of the UHI impacts.

2.3.1. The Normalized Difference Vegetation Index (NDVI)

The Normalized Difference Vegetation Index (NDVI) is calculated from the visible red and near infrared bands. The rationale of the index is that healthy vegetation has a high reflectance in the near infrared (NIR) and a low reflectance in the red, thereby enhancing the interpretation of vegetation cover while suppressing subtle noise from other land cover types. The NDVI can be calculated as (1).

$$\mathrm{NDVI} = \left((\mathrm{IR} - \mathrm{R}) / (\mathrm{IR} + \mathrm{R})\right) \quad (1)$$

Where:
NDVI = Normalized Vegetation Index;
R = Red band of the LANDSAT Image; and
IR = Infrared band of the LANDSAT Image

In this study, the NDVI is calculated for two fundamental reasons, i.e., understanding the city's vegetation pattern and extracting emissivity values. First, the NDVI values indicate whether the land cover type is vegetation, which has been shown to have a cooling effect on surfaces temperatures, hence adopted as the UHI mitigation strategies. Secondly, the NDVI was also used to derive emissivity values from the LANDSAT data based on their mutual direct relationship. The emissivity values are critical parameters needed for modeling the LST from the LANDSAT TM6 image.

2.3.2. The Normalized Difference Built-up Index

The Normalized Difference Built-up Index (NDBI) has been an effective technique to map built-up areas with accuracy of 92% [15]. The index counts on the reflectivity of urban buildings, which is higher in the fifth band and lower in the fourth band and hence is calculated as:

$$\mathrm{NDBI} = \left(\mathrm{MIR} - \mathrm{NIR}\right) / \left(\mathrm{MIR} + \mathrm{NIR}\right) \quad (2)$$

Where:
NDBI = Normalized Difference Built-up Index;
MIR = Middle Infrared Band of the LANDSAT Image; and
NIR = Near Infrared of the LANDSAT Image

The NDVI and NDBI were used to establish a correlation matrix with the LST. Based on their theoretical relation, the three variables were used as a second way of empirically validating the values of the LST modeled by the mono-window algorithm [19].

2.3.3. Retrieving the Land Surface Temperature (LST)

The LANDSAT TM6 is a thermal-infrared (TIR) band (10.40 to 12.50 μm) that has been commonly used for the LST mapping. For this study, the mono-window algorithm [19] was used to retrieve the LST. The mono-window algorithm [19] is based on a thermal radiance transfer equation and requires three parameters: emissivity, transmittance and effective mean atmospheric temperature, to retrieve the LST from the LANDSAT TM6. The algorithm can be written as:

$$\mathrm{Ts} = \left\{ a(1 - C - D) + \begin{bmatrix} b(1 - C - D) \\ + C + D \end{bmatrix} Ti - DT_a \right\} / C \quad (3)$$

Where:
Ts = is the Land surface temperature (^{o}K);
a = −67.355351
C = εi × τi ; and D = (1 − τi) [1 + (1 − εi) × τi] such that
εi = is the emissivity,
τi = is the atmospheric transmittance,
b = 0.458606
T_i= is the brightness temperature of TM6 image (K^{o}).
T_a = represents the effective mean atmospheric temperature (K^{o}).

Therefore, according to equation (3), the remainder of this section discusses how variables of mono-window algorithm [19] were obtained. These are brightness temperature of TM6 image (Ti) in degree Kelvin; atmospheric transmittance (τi); effective mean atmospheric temperature (Ta); and land surface emissivity (εi).

The brightness temperature of TM6 image (Ti), also known as at-sensor (radiance) temperature, is calculated in a two-step process. First, the digital number is converted into spectral radiance. The LANDSAT TM sensors acquire temperature data in TM6, and store the information as digital numbers whose values range between 0 and 255. The numbers are converted into spectral radiances by the following equation:

$$\mathrm{L} = \mathrm{LMIN} + \left(\mathrm{LMAX} - \mathrm{LMIN}\right) * \mathrm{DN} / 255 \quad (4)$$

Where:
L = Spectral radiance
LMIN = 1.238 (Spectral radiance of DN value 1)
LMAX = 15.600 (Spectral radiance of DN value 255)
DN = Digital Number (image's brightness value)

Secondly, the spectral radiances are converted into degree Kelvin by the help of Planck's function, shown as:

$$\mathrm{T_i} = \mathrm{K_2} / \ln\left(1 + \mathrm{K_1} / \mathrm{L}\right) \quad (5)$$

Where:
L = Spectral radiance
K_1= Constant 1 = 60.776 MW*cm^{-2} *sr^{-1} * μm^{-1}
K_2 = Constant 2= 1260.56^{0}K
T_i = is the brightness temperature of TM6 image i.e., at sensor Temperature in ^{o}K

However, there is a difference between values of at-sensor and ground temperatures, because of the attenuation caused by the atmosphere. Hence, the atmospheric transmittance is calculated to account for this attenuation. The atmospheric transmittance was calculated using a two-step process. First, the atmosphere's water vapor content was derived from the relative humidity (RH) and the near-surface temperature. The equation for deriving the water vapor content is given by:

$$W_i = 0.0981 * \left\{ \begin{array}{l} 10 * 0.16108 \\ * \exp\left\{ \begin{array}{l} 17.27 * (T_o - 273.15) \\ 237.3 + (T_o - 273.15) \end{array} \right\} \\ * RH \end{array} \right\} + 0.1697 \quad (6)$$

Where:
W_i = is the water vapor content (g/cm2);
T_o = is the near-surface air temperature in ^{o}K and

RH = represents the relative humidity.

Secondly, once the water vapor content was calculated, the atmospheric transmittance was estimated with the following equations [19,20] in Table 2.

$$\tau i = 1.031412 - 0.11536 * Wi \quad (7)$$

Where:

τ_i = is the atmospheric transmittance of LANDSAT TM 6 and

Wi = represents the water vapor content

Table 2. Equations of calculating Atmospheric Transmittance as a function of Water Vapor Content of the Air column (profile) [19,20]

Air Column (Profile)	Water vapor content (w) (g/cm^2)	Atmospheric Transmittance Equation
High air temperature	0.4 -1.6	0.974290 - 0.08007 w
High air temperature	1.6 – 3	1.031412 - 0.11536 w
Low air temperature	0.4 -1.6	0.982007 - 0.09611 w
Low air temperature	1.6 – 3	1.053710 - 0.14142 w

Finally, the mean atmospheric temperature (Ta) was estimated from near surface air temperature based on regional conversion formula proposed [19,20] (See Table 2). The near surface temperature in degree Kelvin is Chicago air temperature recorded at the time of satellite overpass. Accordingly the mean aerial temperature of Chicago was given by:

$$T_a = 25.9396 + 0.88045 T_0 \quad (8)$$

Where:

T_a = Effective mean aerial temperature of Chicago (^{o}K)

T_0 = near surface air temperature (^{o}K)

The LST is also a factor of the land surface emissivity, which is the efficiency of transmitting thermal energy across the surface into the atmosphere. The land surface emissivity (εi) is estimated by using the NDVI. For the NDVIs between 0.157 and 0.727, the land surface emissivity is calculated with equation (9) [23]. Table 4 contains equations for complete land surface emissivity estimation with the NDVI data.

$$\varepsilon i = 1.009 + 0.0047 Ln(NDVI) \quad (9)$$

Where:

εi = Land surface emissivity

NDVI = Normalized Difference Vegetation Index

Table 3. Table containing a formula for emissivity calculation from NDVI [15]

NDVI	NDVI < −0.185	−0.185 ≤ NDVI < 0.157	0.157 ≤ NDVI ≤ 0.727	NDVI > 0.727
Emissivity	0.995	0.97	=1.009+.047ln(NDVI)	0.99

2.3.4. Model Validation

The NDBI and NDVI were used for the verification of the modeled LST values. Both qualitative and quantitative validation methods are used for verification. Qualitatively, visual interpretations and comparisons of the images of the NDBI, NDVI and LST values were done. A correlation matrix was used for the quantitative evaluation. Theoretically, the LST values must have a positive relationship with the NDBI values and a negative relationship with the NDVI values.

2.3.5. The Urban Thermal Field Variance Index

Several thermal comfort indices are available for evaluating the UHI impacts on the urban quality of life. These are the Temperature Humidity Index (THI) [24], the Physiological Equivalent Temperature (PET) [25], the Wet-bulb Globe temperature (WBGT) [26] and the Urban Thermal Field Variance Index (UTFVI) [14]. In this study, the UTFVI is used for the ecological evaluation of Chicago's urban heat island because of its prior tested application to the LANDSAT data. The UTFVI values were classified into six categories, each having corresponding interpreted ecological valuations and the UHI phenomenon [18]. The index, which analyzes the UHI effect on the quality of urban life, is calculated using equation (10) as follows:

$$UTFVI = \left(T_S - T_{mean}\right) / T_{mean} \quad (10)$$

Where:

UTFVI = Urban Thermal Field Variance Index

T_S = LST (^{o}K)

T_M = Mean LST (^{o}K).

3. Results and Discussion

3.1. The Accuracy Verification of LST Retrieval

The qualitative visual interpretation of the images of the NDBI, NDVI and LST values verified the theoretical relationships of these variables (Figure 2). Accordingly, areas with the high NDVI values (e.g., parks) have the low NDBI values and the low LST (LST< 32 °C). On the other hand, waterbodies while having the low NDVI (NDVI< 0), also have the low LST (i.e., < 26 °C) and the NDBI. Built-up areas, which had the high NDBI, as expected, also had the low NDVI and the high LST (i.t., > 35 °C).

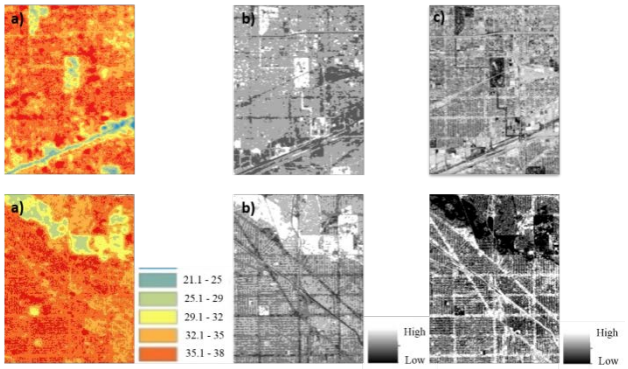

Figure 2. The LST values and corresponding NDVI and NDBI values for the same areas, a) LST values from 21 to 38 °C, B) NDVI values from -1 to 1, C) NDBI values from -1 to 1

Furthermore, the quantitative evaluations of the LST, NDVI and NDBI images, through correlation matrix, also depicted similar outcomes (See Table 4.) According to the matrix, the highest relationship (i.e., r = -0.9) was observed between the NDBI and NDVI images. The high negative correlation between the NDBI and NDVI images is indicative of waning vegetation cover as the land use changes into built-up areas. On the other hand, the relationship between the LST and NDBI images is r = 0.26, while that of the LST and NDVI images is r = -0.34.

Although the magnitudes of the relationships were not as strong, the direction is revealing. The positive relationship of the LST and NDBI values reveals the heating impact of built-up and impervious surface areas on surface temperature, while the negative relationship of the LST and NDVI values ascertained the cooling impact of forests, woodlands, parks, and other city green spaces. The direction of the relationship captured by the correlation matrix is significant, as correlation matrix was generated through pixel-based comparison, where confounding subtle noises in the data would obscure chances of obtaining revealing relationships.

Table 4. Correlation matrix of LST, NDVI and NDBI of Chicago city after masking the water bodies

	LST	NDVI	NDBI
LST	1.00	-0.34	0.26
NDVI	-0.34	1.00	-0.90
NDBI	0.26	-0.90	1.00

Several previous studies have shown a comparable relationship between the LST values and these indices [28,29,30]. For instance, a negative relationship (i.e., r = 0.6) is documented between the NDVI and LST, until the NDVI reaches a threshold value of 0.6 [29]. It is not quite clear why the cooling effect of the natural vegetation decimates when the percent canopy cover increases beyond this threshold value. And yet the negative correlation between the NDVI and LST indicate the effect of vegetation in reducing the UHI effect, thereby reassuring its utility for UHI mitigation. On the other hand, the positive NDBI and LST relation [30] indicated the logical association of the built-up areas and UHI. Both uncrowned settlement pattern, greening urban spaces and increasing the albedo (i.e., reflection coefficient) of the built-up surfaces can be adopted to lessen the impacts of the UHI in Chicago.

3.2. Analysis of Urban Heat Islands (UHI) of Chicago

The spatial distribution of the LST of Chicago is shown in Figure 3. According to the result, the mean LST is 33.6°C, the maximum and minimum LSTs are 16°C and 44°C, respectively. The higher LST dominates northwestern areas of the city, while the eastern and southern areas have the lower LST. The UHI impacts of built-up areas were found to depend on the density of settlement with medium sized building. In Chicago, neighborhoods on the South Side are less crowded and have noticeable green spaces as compared with neighborhoods to the north perhaps hinting as to why the LST in the northern areas were higher vis-à-vis the South Side. The results verify a previous US EPA UHI project [17], which reported a consistent high UHI intensity in northwestern Chicagoland as compared to the east and downtown area. The presence of Lake Michigan in the east and southeast are believed to have moderated the local microclimate. Additionally, it could be because of a low Sky View Factor (SVF), i.e., a relatively cooler air temperature from the shedding effect of densely populated skyscrapers around downtown Chicago.

In general, the largest portion of Chicago (i.e., 41.3%) experiences the LSTs around 32 to 35°C. This was found mainly in areas close to Lake Michigan and the wider residential areas. The second largest LST class is 35-38°C, and constitutes about 28.9% of the city, mainly in the north and northwestern areas. The hottest LST (i.e., 38°C and above) is experienced in relatively small pocket areas (i.e., 4.2%) of Chicago, mainly where the large industrial buildings and train stations are located. The high UHI detected in areas of large industrial complexes and train stations, maybe indicating the possible air heating impacts of steams and smokes coming out of the industrial plants and the concentration of steels and concretes from which railroad stations are made. On the other hand, the lowest LST (less than 26°C) recorded in only 2% of the city mainly on the lands covered by water (i.e., lakes and wetlands). Areas having the LSTs between (26 - 29°C) constitute 5.8% of the landscape, and these are lands in close proximity to the Lake Michigan, forest areas and parks. The remaining 17% of Chicago has the LSTs between 29°C and 32°C, mainly on lands that are occupied by forest vegetation, woodlands and green spaces.

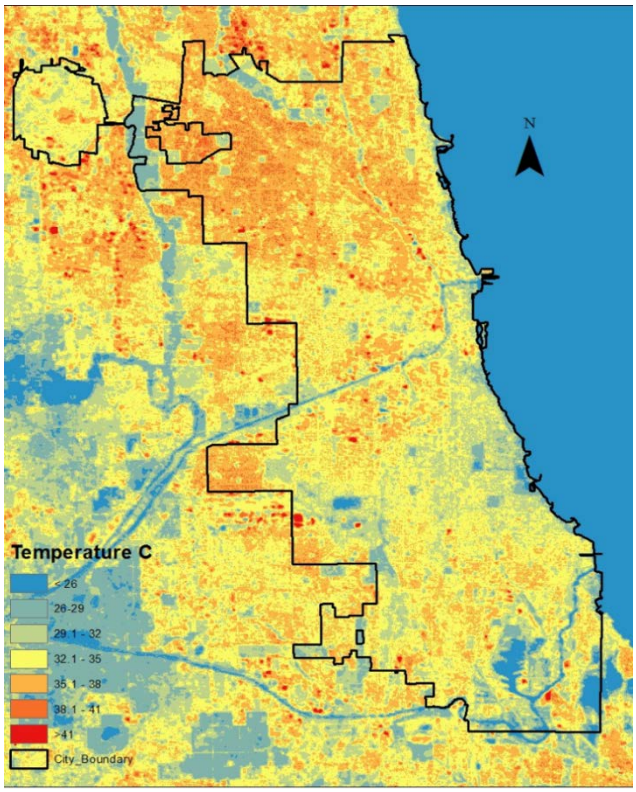

Figure 3. Land Surface Temperature (LST) distribution in Chicago city on May, 2010 in degree Celsius, derived from LANDSAT images using mono-window algorithm. Divided into seven classes, each class is one standard deviation far from the mean

3.3. The Ecological Evaluation of Chicago Urban Heat Islands

The quantitative ecological evaluation of the UHI effects in Chicago is shown in Figure 4. According to the Urban Thermal Field Variance Index (UTFVI) [14], which measures urban ecological quality of life in terms of the degree of thermal comfort in relation to the existence of the UHI phenomenon, varying impacts of the UHI were detected in Chicago. The city has the two extremes: areas of heat stresses (i.e., UTFVI > 0.02) and areas optimal microclimate (i.e., UTFVI <0) (Figure 4 and Table 5). The

largest portion of Chicago (i.e., 31%) experiences optimal thermal condition (i.e., UTFVI <0) for living. These are downtown areas and locations in close proximity to the Lake Michigan, wetlands, forest and woodlands, parks and green spaces. On the other hand, the areas that are hit by the worse UHI effects (i.e., UTFVI > 0.01) are relatively small pocket areas (i.e., 9%) of Chicago; while those experiencing bad thermal comfort accounts for 16%. In general, according to the ecological evaluation of the UHI effects, the urban thermal field variance index did not detect thermal discomfort on 75% of the city. It was only in the remaining 25% of the city that varying degrees of thermal discomfort and heat stresses were detected.

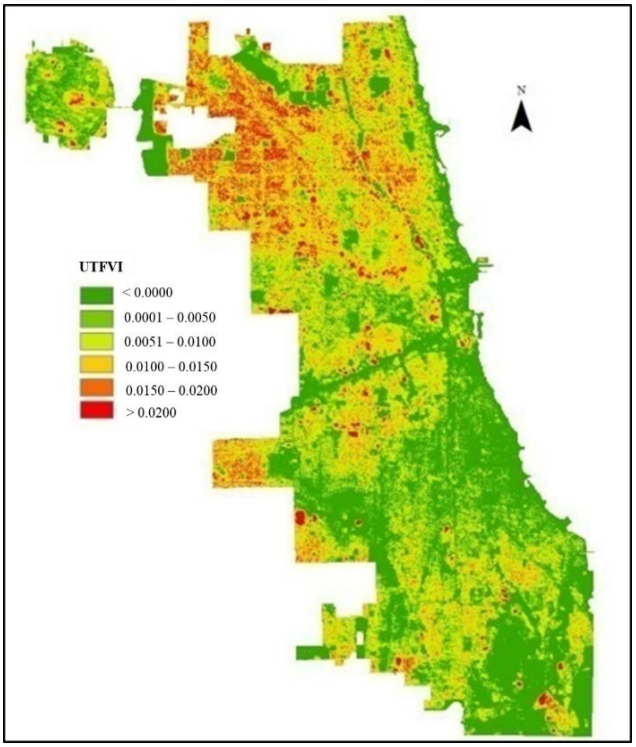

Figure 4. Ecological evaluation index of Chicago city in May 2010, according to thermal field variance index (UTFVI)

In general, regional analysis of Chicago's UHI and UTFVI conforms to studies that analyzed spatiotemporal patterns of the UHI in metropolitan Shanghai [31] and Western Territories of Hong Kong [27]. According to the study in Shanghai, urban parks were, on average, 4.5°C cooler than the surroundings city areas [31]; whereas in the Western Territories of Hong Kong, similar strong association between the LST and LULC types is reported. In the Western Territories of Hong Kong, urban parks and woodlands had similar air temperature as undeveloped rural vegetated areas [27]. Moreover, this study corroborates a report of Chicago's UHI Policy implications, post-1995 heat wave [6]. According to the report, even if there is a reduction in the UHI intensity, because of the city's UHI mitigation strategies, northwestern and pockets of areas in southern and southeastern Chicago are still experiencing the UHI stresses. Therefore, urban planning that pursues spacious settlement pattern with green spaces and parks, and wetlands preservation is important to strengthen Chicago's UHI mitigation strategies and thereby to maintain urban quality of life.

Table 5. The interpretation of the index quantitative evaluating of the ecological effects of the Chicago city Urban Heat Island (UHI) [18]

Urban thermal field variance index	Urban heat island Phenomenon	Ecological evaluation Index
Less than 0	None	Excellent
From 0 to 0.005	Weak	Good
From 0.005 to 0.01	Middle	Normal
From 0.01 to 0.015	Strong	Bad
From 0.015 to 0.02	Stronger	Worse
More than 0.02	Strongest	Worst

4. Conclusion

The LST, extracted from the 2010 LANDSAT TM6 using mono-window algorithm, indicated varying distribution of the UHI phenomenon in Chicago city. In general, there was a difference of 18°C between the low UHI intensity areas around the Lake Michigan in the east and the high intensity areas in the densely populated northwestern neighborhoods. Mainly the distribution of the UHI phenomena were found to have a direct relationship to the city's land use/land cover distribution. By and large, while waterbodies, forest and woodlands, urban parks and green spaces, and skyscrapers have lowered the phenomena of UHIs; densely populated buildings, congested settlement, industrial zones and large train stations have intensified the UHI effects.

According to Chicago's UTFVI, which measured the urban ecological quality of life via the relationship of thermal comfort and the UHI instensity values, ranges of thermal comforts were detected. The city experiences both extreme conditions of optimal microclimate for quality urban life and the worst condition of thermal discomfort. Seventy-five percent of the city's landscape experiences normal to excellent microclimate for living, which is encouraging. This is perhaps due to the cooling effects of the Lake Michigan, the downtown's high-rise buildings, and the city's mitigation responses adopted after the 1995 heat wave. However, a bad-to-worse heat stress condition is detected in sizable portion of the city (i.e., 25%), indicating potential impacts of the UHI phenomenon on urban quality of life, particularly in northwestern neighborhoods and small pocket areas in the south and southeast. It is therefore important for the city to strengthen and expand the hitherto adapted UHI mitigation strategies to maintain quality urban life for Chicago residents.

Acknowledgement

The authors are grateful to anonymous reviewers, whose feedback have improved the content and presentation of the manuscript. Also the authors thank the following institutions for providing the main and ancillary data for this study: U.S. Geological Survey (USGS), Weather Underground Inc., and Chicago State University (CSU). Also the authors are indebted to CSU's GIS laboratory for software provision and technical support; and Ms. Gabrielle Toth, CSU Librarian for proofreading the manuscript.

References

[1] United Nations, Department of Economic and Social Affairs, Population Division, *World Urbanization Prospects: The 2014 Revision*, (ST/ESA/SER.A/366)(2015).

[2] WHO, *World health statistics 2016: monitoring health for the SDGs, sustainable development goals*, World Health Organization, Geneva, Switzerland, (2016).

[3] E.J. Gago. , J. Roldan, R. Pacheco-Torres, J. Ordóñez, The city and urban heat islands: A review of strategies to mitigate adverse effects, *Renewable and Sustainable Energy Reviews* 25: 749-758, (2013).

[4] K. W., Oleson , A. Monaghan, O. Wilhelmi, M. Barlage, N. Brunsell, J. Feddema, L. Hu, D. F. Steinhoff, Interactions between urbanization, heat stress, and climate change, *Climatic Change* 129 (3) 525-541, (2005).

[5] U.S. Environmental Protection Agency, Climate change indicators in the United States, 2014. Third edition. EPA 430-R-14-004, (2014).

[6] C. W. Mackey, X. Lee, and R. B. Smith, Remotely sensing the cooling effects of city scale efforts to reduce urban heat island, *Building and Environment* 49: 348-358, (2012).

[7] Coseo P. and L. Larsen, How factors of land use/land cover, building configuration, and adjacent heat sources and sinks explain Urban Heat Islands in Chicago, *Landscape and Urban Planning* 125: 117-129, (2014).

[8] T. Friehat, G. Mulugeta, and T. S. Gala, "Modeling Urban Sprawls in Northeastern Illinois." Journal of Geosciences and Geomatics, vol. 3, no. 5 (2015).

[9] K.A. Gray, and Finster, M.E., *The Urban Heat Island, Photochemical Smog, and Chicago: Local Features and the Problem and Solution. Northeastern University, Evanston, IL*., Available from: http://www.epa.gov/hiri/resources/pdf/post_chicago/chicago_toc_exsum.pdf., (2000).

[10] J. E, Dematte,. Karen O'Mara; Jennifer Buescher ; Cynthia G. Whitney; Sean Forsythe; Turi McNamee; Raghavendra B. Adiga, ; and I. Maurice Ndukwu, Near-Fatal Heat Stroke during the 1995 Heat Wave in Chicago, *Annals of Internal Medicine* 129 (3): 173-181. (1998).

[11] R. Kaiser, Alain Le Tertre, Joel Schwartz, Carol A. Gotway, W. Randolph Daley, and Carol H. Rubin, The Effect of the 1995 Heat Wave in Chicago on All-Cause and Cause-Specific Mortality, *American Journal of Public Health* 97(1) 158-162, (2007).

[12] B., Ackerman, Temporal march of the Chicago heat island. *J. Climate Appl. Meteor.*, 24, 547-554, (1985).

[13] K.R., Smith and P.J, Roebber, Green Roof Mitigation Potential for a Proxy Future Climate Scenario in Chicago, Illinois, *Journal of Applied Meteorology and Climatology* 50:3, 507-522, (2011).

[14] Y. Zhang, Land surface temperature retrieval from CBERS-02 IRMSS thermal infrared data and its applications in quantitative analysis of urban heat island effect, *J. Remote Sens.* 10: 789-797, (2006).

[15] H. Z. Zhang , Q.X. Ye, Y, Cai, W. Ma, and M. Chen, Analysis of land use/land cover change, population shift, and their effects on spatiotemporal patterns of urban heat islands in metropolitan Shanghai, China, *Applied Geography* 44: 121-133, (2013).

[16] U.S Census. *Census Bureau, U.S. Department of Commerce*, November (2014), Available from http://www.census.gov/.

[17] U.S. EPA *Urban Heat Island Project* (2002). Profile of Chicago, Available at URL: http://epa.gov/heatisl/pilot/archies/chicago.pdf.

[18] L. Liu and Y. Zhang, Urban Heat Island Analysis Using the Landsat TM Data and ASTER Data: A Case Study in Hong Kong, *Remote Sens.*3:1535-1552, (2011).

[19] Z. Qin, Zhang, M.; Amon, K; Pedro, Mono-window Algorithm for retrieving land surface temperature from Landsat TM 6 data, *Acta Geogr. Sinica* 56: 456-466, (2001).

[20] Z. L., Lia, H. W. , Ning Wanga, S. Qiub , J. A. Sobrinod, Z. Wane , B. H., Tanga , and G. Yanf, Land surface emissivity retrieval from satellite data, *International Journal of Remote Sensing* 34 (9-10) 3084-3127 (2013).

[21] A.R. Gillespie, Rokugawa, S.; Matsunaga, T.; Cothern, J.S.; Hook, S.J.; A.B., Kahle, temperature and emissivity separation algorithm for advanced spaceborne thermal emission and reflection radiometer (ASTER) images, *IEEE Trans. Geosci. Remote Sens.* 36: 1113-1126, (1998).

[22] J.C., Jimenez-Munoz, J.A. Sobrino, A generalized single-channel method for retrieving land surface temperature from remote sensing data, *J. Geophys. Res.* 108: 4688-4694, (2003).

[23] A.A. Van de Griend, M. Owe, On the relationship between thermal emissivity and the normalized difference vegetation index for natural surfaces. *Int. J. Remote Sens. 14*:1119-1131, (2003).

[24] A.N., Kakon M. Nobuo, S. Kojima, T. Yoko, Assessment of thermal comfort in respect to building height in a high-density city in the tropics, *Am. J. Eng. Appl. Sci.*, 3 (3): 545-551, (2010).

[25] A. Matzarakis, H. Mayer, M.G. Iziomon, Applications of a universal thermal index: physiological equivalent temperature, Int. *J. Biometeorol.*, 43 (2): 76-84, (1999).

[26] K. M. Willett, S. Sherwood, Exceedance of heat index thresholds for 15 regions under a warming climate using the wet-bulb globe temperature. *Int. J. Climatol.*, 32 (2): 161-177 (2012)

[27] J. E. Nichol, Remote Sensing of Urban Heat Islands by Day and Night, *Photogrammetric engineering and remote sensing*, 19,1639-1649, (2005).

[28] K. P. Gallo, and T. W. Owen, Assessment of urban heat islands: A multi sensor perspective for the Dallas Ft Worth, USA region, *Geocarto International*, 13: 35-41, (1998).

[29] H. Li, and Q. Liu, Comparison of NDBI and NDVI as indicators of surface urban heat island effect in MODIS imagery, *International Conference on Earth Observation Data Processing and Analysis (ICEODPA)*, SPIE Vol. 7285, 728503(2010).

[30] X.L. Chen, H. Zhao, P. X. Li, Z. Y Yin, Remote sensing image-based analysis of the relationship between urban heat island and land use/cover changes, *Remote Sensing of Environment*104, 133-146, (2006).

[31] Z. L. Li, H. W. Ning, W. Shi., J. A. Sobrino, Z. Wan, B. H. Tang and G. Yan, Land surface emissivity retrieval from satellite data, *International Journal of Remote Sensing*, 34 (9-10) 3084-3127 (2013).